AAS 98-384

MARS GLOBAL SURVEYOR NAVIGATION AND AEROBRAKING AT MARS

P. Esposito, V. Alwar, S. Demcak, E. Graat, M. Johnston and R. Mase
Jet Propulsion Laboratory, California Institute of Technology
4800 Oak Grove Drive
Pasadena, California 91109, USA
E-mail: Pasquale.B.Esposito@jpl.nasa.gov
Phone: (818) 393-1264; Fax: (818) 393-3147

The Mars Global Surveyor (MGS) spacecraft was successfully inserted into an elliptical orbit around Mars on 9/12/97, 01:53:49 UTC. This orbit was near polar (inclination=93.26 deg) with an orbital period of 44.993 hours and apoapsis and periapsis altitudes of 54,025.9 km and 262.9 km respectively. After a short aerobraking (AB) initiation interval (9/12/97 to 10/2/97), the main phase of AB or orbit period reduction was established. However shortly thereafter, a significant problem with the minus-Y axis solar array developed which necessitated a temporary suspension of AB. Ultimately, this forced the Project to abandon the original plan to complete AB on 1/18/98 and establish the mapping orbit on 3/15/98.

The revised plan called for a reduced level of AB, thus subjecting the solar array and yoke assembly to less aerodynamic stress. After 201 orbits and 196 days after MOI, the first phase of AB has ended; the orbital period was 11.64 hours with apoapsis and periapsis altitudes of 17,870.3 and 170.7 km respectively. At present, MGS is in a science phasing orbit (SPO) and shall acquire science data from 3/28/98 to 9/11/98. Thereafter the second phase of AB shall begin and is expected to end during Feb 1999 when the orbital period shall be 1.9 hours and the orbit's descending node shall be at the 2:00 am (local mean solar time) orientation.

MARS ORBIT INSERTION AND CAPTURE ORBIT ACCURACY

The Mars Global Surveyor (MGS) spacecraft was successfully inserted into an elliptical orbit around Mars on 9/12/97, 01:53:49 UTC. This was accomplished by accurate orbit determination establishing the Mars approach trajectory and precise control of the spacecraft during the main-engine, Mars orbit insertion (MOI) burn. The velocity-change specified by the Navigation Team was accomplished as a "pitch-over" maneuver. Thus, the thrust vector was directed along the spacecraft's anti-velocity vector throughout the burn. A pitch-rate of 1.21 deg/min was specified for the burn duration resulting in a 27.5 deg burn, angular arc centered on periapsis. This procedure was adopted in order to improve the efficiency of this maneuver. It saved the equivalent of 20 m/s in propellant as compared to an inertially-fixed attitude. The implementation of the MOI burn involved a 20 sec ullage burn using a series of eight small thrusters, with an effective thrust of 31.1 N, followed by

a 1339.7 sec firing of the main engine, with an effective thrust of 655.3 N. The braking velocity-change was 973.0 m/sec. Both targeted and achieved capture orbital elements are specified in Table 1. This paper provides a continuation of the state of navigation activities; interplanetary phase results were presented in Ref. 1.

Table 1
MGS MARS ORBIT INSERTION RESULTS

Orbit Element	Target Value	Achieved Value
Period, hours	45.0	44.993
Periapsis altitude, km	250.0	262.9
Inclination, deg	93.3	93.258

AEROBRAKING INITIALIZATION

With the capture orbit established, we now initialized aerobraking by gently stepping into the atmosphere, by lowering the periapsis altitude, by a series of small propulsive maneuvers executed at apoapsis. Our orbit numbering procedure identified the first periapsis which occurred during the MOI maneuver as P1. Thus, orbit one started at P1, goes through the first apoapsis, A1, and ends at the second periapsis, P2. A series of six AB initialization maneuvers occurred as shown in Table 2. Given are the velocity-change magnitude for each maneuver, the resulting periapsis altitude and an estimate of the atmospheric density and dynamic pressure at the altitude shown. The densities were derived from an analysis of approximately one orbit of two-way, coherent doppler data. This completed the initialization or walk-in phase; the next AB phase, called the main phase, was defined by a dynamic pressure corridor with upper and lower limits being 0.68 N/m^2 and 0.58 N/m^2 respectively. The upper limit provided for adequate orbit period reduction and safety against aerodynamic heating of critical spacecraft components. The lower limit insured a minimum level of orbit period reduction. Ref. 2 provides the basis for the AB design and planning implemented during flight operations.

Two basic requirements were levied on navigation to insure that MGS was in the correct attitude throughout the drag pass and to guard against unexpected, intrinsic density variation from periapsis to periapsis. These were a) predict the time of periapsis-passage (Tp) to within 225 seconds and b) predict the altitude at periapsis-passage (hp) to within 1.5 km.

Table 2
INITIALIZATION OF AEROBRAKING: THE WALK-IN PHASE

Apoapsis and Walk-in Maneuver	Velocity-Change Magnitude (m/sec)	Resultant Periapsis Altitude (km)	Atmospheric Density and Dynamic Pressure at Periapsis (kg/km^3; N/m^2)
3 AB-1	4.4	149.3	0.36; 0.00 at P4
4 AB-2	0.8	128.4	5.61; 0.06 at P5
5 AB-3	0.3	121.4	10.7; 0.12 at P6
7 AB-4	0.2	116.1	20.1; 0.23 at P8
10 AB-5	0.2	111.2	42.2; 0.49 at P11
11 AB-6	0.05	110.5	45.7; 0.53 at P12

MAIN PHASE AEROBRAKING AND TEMPORARY SUSPENSION

The main phase of AB began with P12 on 10/2/97. During P12 through P15, the orbital period decreased on average by 75.1 min per pass or from 40.4 hours to 36.4 hours due to AB. However, during these periapses, a problem was detected with one of the solar arrays; the minus-Y axis, solar array was deflecting more than was expected as MGS was going through periapsis-passage. During this time, the plus-Y axis, solar array behaved normally. In order to proceed prudently, the Project decided to reduce the AB induced pressure on the solar array and thus the periapsis altitude was increased by 11.0 km with a maneuver at A15. During P16 through P18, the solar array problem persisted and a decision was made to raise the periapsis altitude out of the atmosphere. On A18, this maneuver was performed which increased the altitude to 171.7 km at the following periapsis. MGS remained in this "hiatus orbit" for seventeen orbits (P19 through P36). Mean atmospheric densities were determined for each of these using doppler data and analysis to be described in the next section. After considerable analysis and review of engineering and science data and solar panel ground tests (Ref. 3), AB was resumed with maneuver ABM-3 on 11/7/97. However, the intensity of AB was reduced to a safer level; the new dynamic pressure corridor was 0.15 to 0.25 N/m^2.

Table 3
ABMs EXECUTED TO ESTABLISH THE "HIATUS ORBIT"

Apoapsis and ABM	Velocity-Change Magnitude (m/sec)	Resultant Periapsis Altitude (km)	Atmospheric Density and Dynamic Pressure at Periapsis (kg/km^3; N/m^2)
15 ABM-1	0.5	121.0	17.8; 0.20 at P16
18 ABM-2	2.3	171.7	0.04; 0.00 at P19

WALK-IN AND RE-ESTABLISH THE MAIN PHASE OF AEROBRAKING

A second walk-in strategy was executed similarly to the first walk-in procedure; that is, by slowly reducing the altitude at periapsis by ABMs and assessing the atmospheric density. Once the safety of the spacecraft was assured, another ABM was executed decreasing the periapsis altitude. This continued until a steady level of period reduction (or the dynamic pressure was within the new corridor) was achieved while maintaining safety margins for any stress exerted on the solar array and yoke assembly.

Orbit Analysis Strategy

From MOI until the end of phase 1 AB, orbit determination was performed every orbit by analysis primarily of two-way, coherent doppler and on occasion using one-way doppler (spacecraft to station doppler-shift using the ultra-stable oscillator on the spacecraft as the frequency reference). This was done to a) determine the atmospheric density at periapsis, b) establish a density database for trending and prediction, c) provide the spacecraft team with orbital predictions within the previously stated requirements, d) provide the science teams reconstructed and predicted orbital information for planning and analysis and e) provide the DSN with tracking station angular and doppler-shift predictions. The data acquisition strategy was to acquire a little over one orbit of doppler measurements extending 2-5 hours past periapsis-passage. Because of the spacecraft's

attitude during the drag pass and the geocentric occultation, no tracking data were acquired within approximately one hour centered on periapsis-passage. Range data were acquired occasionally but for Mars ephemeris refinement rather than for orbit determination.

A fiftieth order and degree Mars gravity field model was used as the baseline model in this analysis and is described in Ref. 4. Initial estimates of Mars atmospheric density were determined from the Mars-GRAM (MG) program (Ref. 5). This density information was converted to a static, exponential density model with three input parameters: the base density at the base altitude and the density scale height. Note that other perturbations occurred throughout periapsis-passage, notably spacecraft thrusting in order to maintain spacecraft attitude. Thrusting usually started 5-7 minutes after periapsis and lasted intermittently for about 5 minutes. This effect was modeled initially in our software from telemetry information provided by the spacecraft team. The effective velocity perturbation due to thrusting, usually 1-10 mm/sec, was small compared to that due to the integrated drag effect, approximately 1 m/sec (excluding the hiatus orbits).

In a representative analysis, doppler data were sampled at sixty second intervals. Post-fit doppler residuals generally have a standard deviation of 2.9 mHz (X-band) or 0.051 mm/sec in range-rate.

Atmospheric Density Determination and Orbit Period Reduction

The acceleration due to atmospheric drag was modeled in the navigation software as

$$\ddot{\vec{r}} = -\frac{1}{2}\rho v_r^2 \frac{C_d A}{m}\hat{v}_r \tag{1}$$

with an exponential density model

$$\rho = \rho_o e^{-(h-h_o)/H}. \tag{2}$$

In these equations, C_d is the drag coefficient (= 1.89 initially and 1.99 after P13), A the effective, cross-sectional area of the spacecraft (= 17.02 m^2), m the mass (= 767.8 kg after MOI to 760.4 kg after A201), $\rho(h)$ is the density at altitude h and v_r is the spacecraft's velocity relative to the atmosphere (with the circumflex denoting a unit vector). The base density and base altitude are given by ρ_o and h_o with H being the density scale height. Note that the dynamic pressure is defined as $\rho v_r^2/2$ as in Eq. 1. An estimate of the orbit period change per periapsis passage is given by (Ref. 6)

$$\Delta P = -6\pi\left(\frac{\pi}{2}\right)^{\frac{1}{2}} \frac{C_d A}{m}\rho_p H^{\frac{1}{2}} \frac{a^2}{\mu}\left[\frac{(1+e)^3}{e(1-e)}\right]^{\frac{1}{2}} \tag{3}$$

where ρ_p is the density at periapsis, a and e are the orbit's semi-major axis and eccentricity and μ is Mars' gravitational constant (= 42,828.3 km^3/sec^2). It is clear from Eq. 3 that the periapsis density and scale height will be highly correlated if one attempts to solve for both parameters from a single orbit of data under the data acquisition condition mentioned previously. Also note that for the same density, significantly larger period reduction shall occur early in AB because of the dependence on the square of the semi-major axis.

For every orbit, the base density was estimated, holding the scale height constant, along with other relevant parameters. Based upon the Viking mission results (Ref. 7) and a cooperative collaboration with the MGS accelerometer experiment team (Ref. 8), we used an average scale height of 6.0-7.0 km throughout much of our analysis. This was the basis for the determination of the densities and dynamic pressures given in Tables 2-5 and Figures 1 and 2. The single density near 150 km was evaluated during the initial walk-in and the smaller densities were determined during the hiatus orbits and several orbits in the SPO phase. A mean scale height of 9.0 km was deduced over the altitude range given in Figure 2.

The orbit period reduction due to AB is summarized in Figure 3. Clearly shown is the initial steep rate of period reduction, the suspension of AB and the re-initialization of AB at a reduced level. Figure 4 shows the period change per orbit. The largest period change per orbit, -93.9 min, occurred during P15 when the density was 78.3 kg/km^3 corresponding to a dynamic pressure of 0.90 N/m^2. Note that this figure was truncated at minus 30 min period change in order to clearly resolve smaller changes. From P8 to P15, seven orbits had period reductions greater than 30 minutes.

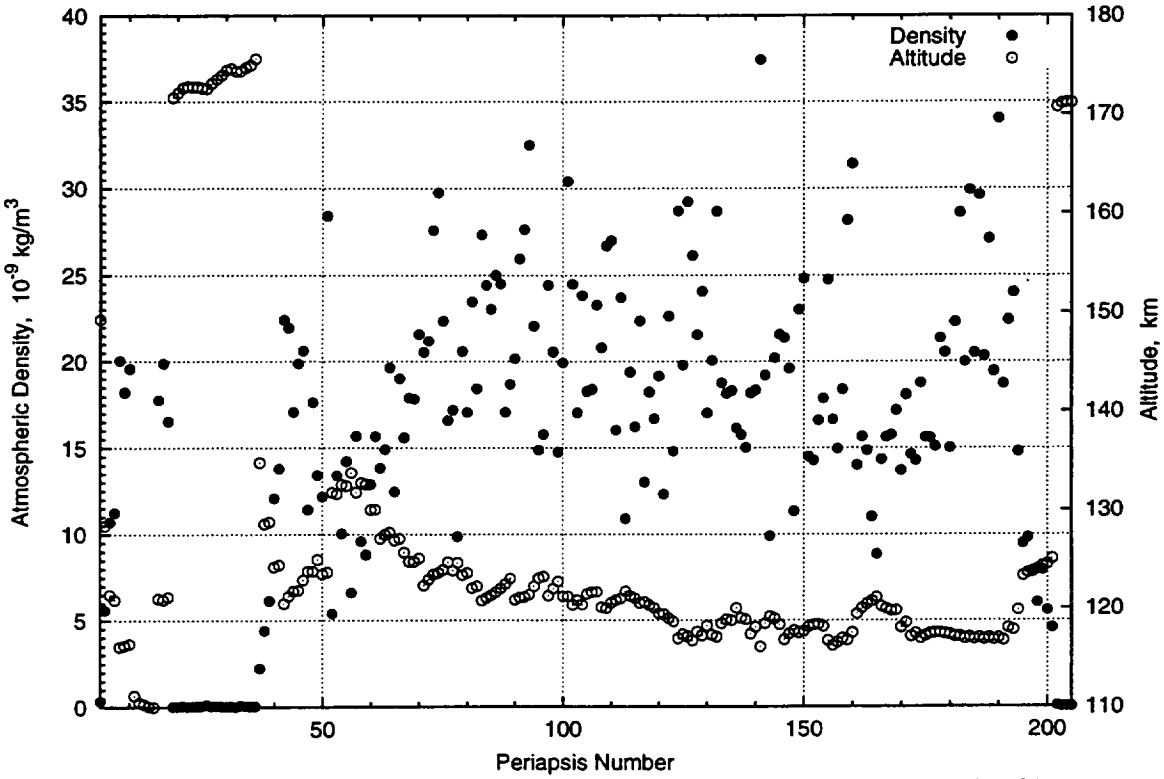

Figure 1 Atmospheric Density At Periapsis Evaluated At The Altitudes Shown Throughout AB Phase 1.

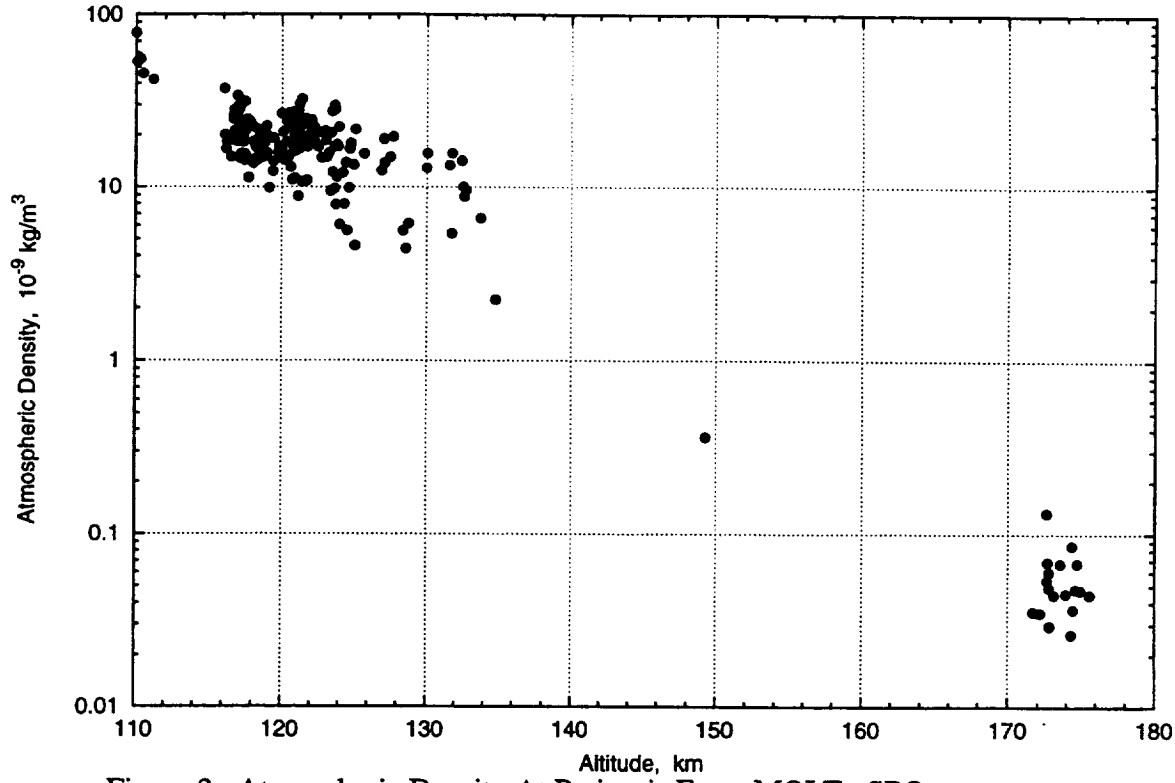

Figure 2 Atmospheric Density At Periapsis From MOI To SPO.

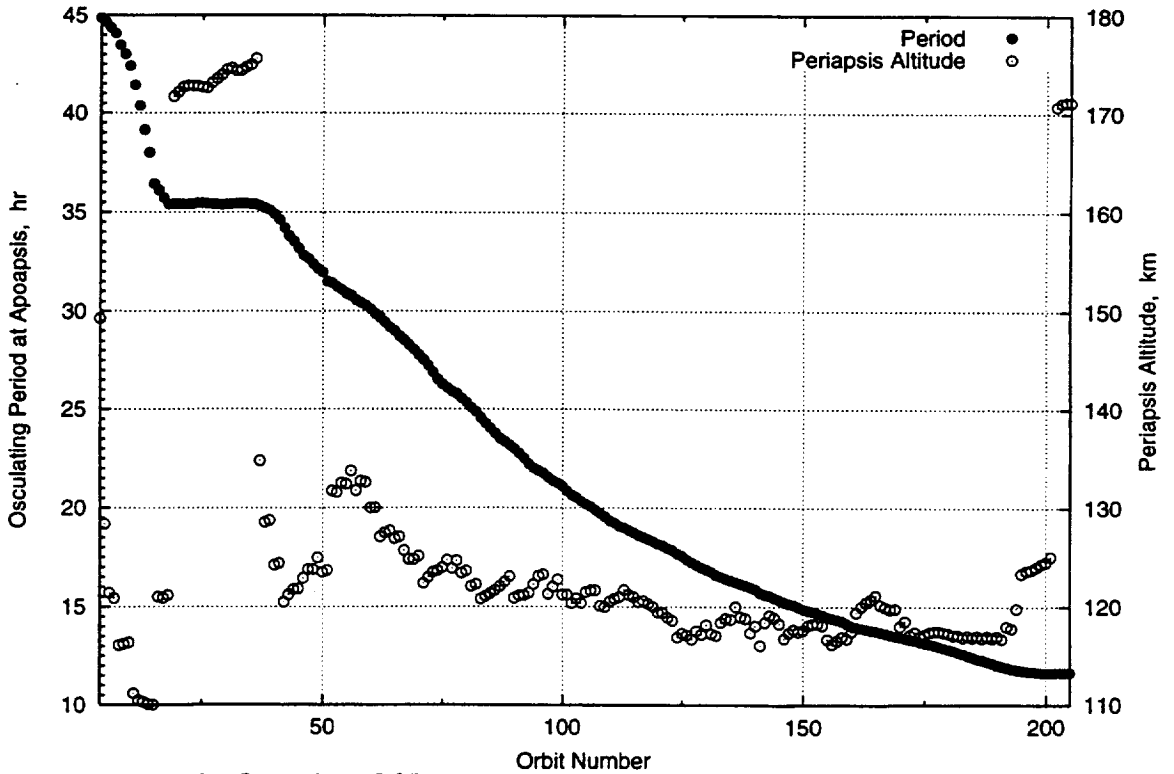

Figure 3 Overview Of Period Reduction With Corresponding Periapsis Altitudes.

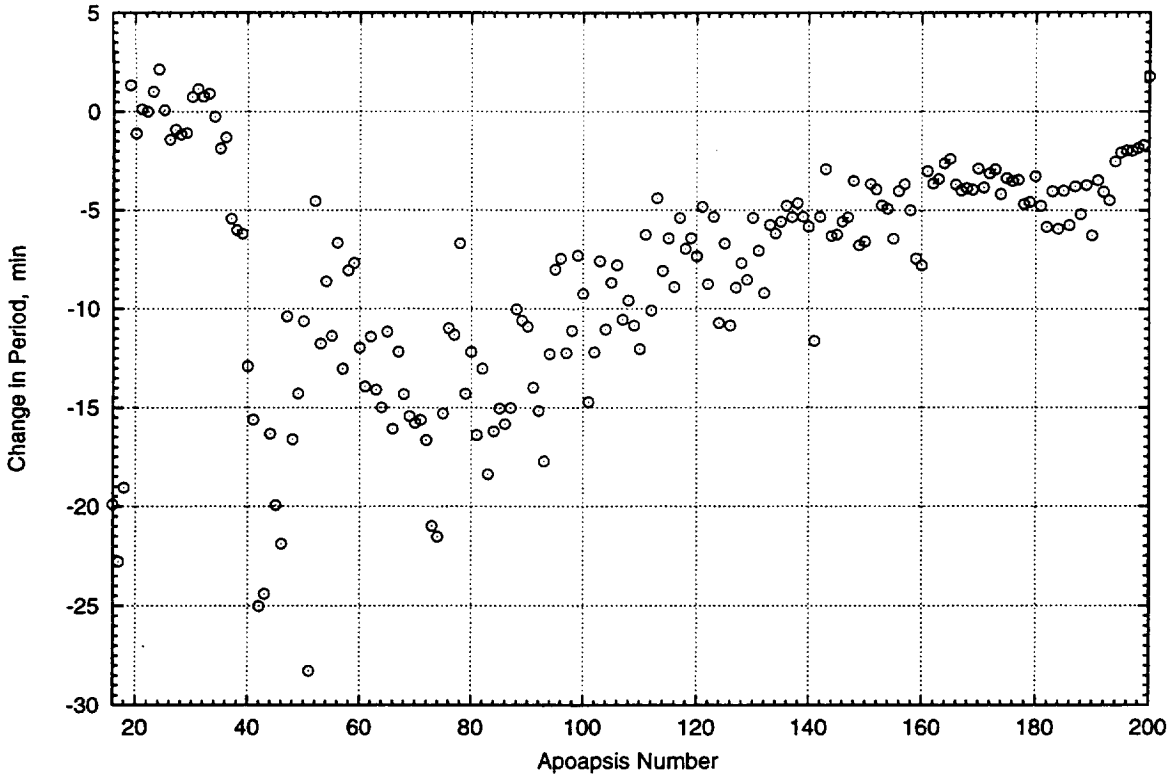

Figure 4 Period Changes Per Orbit During AB.

ABMs - Adjusting the Altitude At Periapsis-Passage For Corridor Control

During the main phase of the revised AB plan, the near term objective was to achieve an 11.64 hour orbit period by 3/22/98 but no later than 4/22/98 near the start of the solar conjunction phase of the mission. While this provided substantial time margin for achieving the objective, an early termination of AB was desirable. This would allow more science data acquisition in the SPO prior to solar conjunction which shall occur on 5/13/98.

In principle, the plan was straightforward. Stay within the dynamic pressure corridor, achieve the expected level of orbit period reduction and terminate AB as scheduled. In practice, difficulties arose because of the uncertainty in predicting the atmospheric density throughout the drag pass even one orbit into the future.

Assembled in Table 4 are all of the AB propulsive maneuvers (ABMs) necessary for MGS to remain within the dynamic pressure (or density or periapsis altitude) corridor established in the overall plan. For the most part, third body perturbations due to the Sun and Mars' gravity field tended to increase hp. As the density decreased, period reduction would be reduced beyond the lower limit necessary to keep AB on schedule. Thus, a "down" ABM would be executed. Some ABMs were executed to increase hp (an "up" ABM) either as a response to a) the Noachis regional dust storm (centered approximately at 0 deg longitude and 40 deg south latitude) on A51 and b) approaching or exceeding the upper limit of the corridor thereby threatening the already weakened solar array assembly. In this table, "up" ABMs are indicated with an asterisk and "+" signs mean the ABM was executed several hours after apoapsis

Table 4

ABMs FOR WALK-IN AND MAIN PHASE AEROBRAKING

Apoapsis and ABM		Velocity-Change Magnitude (m/sec)	Resultant Periapsis Altitude (km)	Atmospheric Density and Dynamic Pressure at Periapsis (kg/km^3; N/m^2)
36	ABM-3	1.9	134.8	2.25; 0.03 at P37
37	ABM-4	0.3	128.6	4.41; 0.05 at P38
39	ABM-5	0.2	124.2	---
39	ABM-6+	0.2	120.2	---
39	ABM-7+	0.5 *	124.2	12.1; 0.14 at P40
41	ABM-8	0.2	120.5	22.4; 0.26 at P42
49	ABM-9	0.1	123.5	12.2; 0.14 at P50
51	ABM-10	0.1 *	---	----
51	ABM-11+	0.25 *	131.7	5.40; 0.06 at P52
56	ABM-12	0.1	131.8	15.7; 0.18 at P57
59	ABM-13	0.2	130.0	12.9; 0.15 at P60
61	ABM-14	0.2	127.1	13.8; 0.16 at P62
64	ABM-15	0.1	126.9	12.5; 0.14 at P65
66	ABM-16	0.1	125.7	15.6; 0.18 at P67
67	ABM-17	0.1	124.8	17.9; 0.20 at P68
70	ABM-18	0.2	122.4	20.6; 0.23 at P71
76	ABM-19	0.1	123.9	17.2; 0.19 at P77
78	ABM-20	0.1	123.4	20.6; 0.23 at P79
80	ABM-21	0.1	122.1	23.5; 0.26 at P81
82	ABM-22	0.1	120.8	27.3; 0.31 at P83
89	ABM-23	0.17	120.9	20.2; 0.23 at P90
96	ABM-24	0.11	121.3	24.4; 0.27 at P97
99	ABM-25	0.11	121.2	19.9; 0.22 at P100
101	ABM-26	0.12	120.4	24.5; 0.27 at P102
106	ABM-27	0.18	121.7	23.3; 0.26 at P107
107	ABM-28	0.18	120.1	20.8; 0.23 at P108
114	ABM-29	0.12	121.0	16.2; 0.18 at P115
116	ABM-30	0.06	120.6	13.0; 0.14 at P117
118	ABM-31	0.13	120.0	16.7; 0.18 at P119
120	ABM-32	0.07	119.4	12.3; 0.14 at P121
122	ABM-33	0.13	118.6	14.8; 0.16 at P123
123	ABM-34	0.13	116.9	28.7; 0.32 at P124
130	ABM-35	0.13	117.3	20.1; 0.22 at P131
136	ABM-36	0.13	119.0	15.8; 0.17 at P137
138	ABM-37	0.23	117.4	18.2; 0.20 at P139
140	ABM-38	0.15	116.1	37.4; 0.41 at P141
141	ABM-39	0.15 *	118.4	19.2; 0.21 at P142
145	ABM-40	0.15	116.8	21.4; 0.23 at P146
154	ABM-41	0.15	116.7	24.8; 0.27 at P155
155	ABM-42	0.08	116.2	16.7; 0.18 at P156
159	ABM-43	0.09 *	117.5	31.4; 0.34 at P160
160	ABM-44	0.17 *	119.4	14.0; 0.15 at P161
165	ABM-45	0.09	120.2	14.3; 0.15 at P166
169	ABM-46	0.17	118.0	13.7; 0.15 at P170
171	ABM-47	0.17	117.1	14.6; 0.16 at P172
173	ABM-48	0.09	117.0	18.8; 0.20 at P174

Atmospheric Density Prediction Using the Mars-GRAM Model

The Navigation Team used the exponential model as the basis for the estimation of the base density from doppler data analysis. Since the base altitude was always chosen to be close to the actual periapsis altitude, this density was essentially a periapsis density. However for predicting densities for future periapsis-passages, we used the Mars-GRAM (MG) model. One significant correction was made to Mars-GRAM based predictions. Based on our estimate of density for past orbits, we trended the density and the following ratio was calculated:

$$f = \text{Navigation determined density / MG predicted density.} \quad (4)$$

From successive orbits, a three orbit, running mean, f-ratio was calculated. Thus the density used in the numerical integration of the drag equations of motion (Eq. 1) was adjusted as follows:

$$\text{density(updated)} = f * \text{density(MG)} \quad (5)$$

thus providing a more accurate density for future predictions. Initially, the MG model was under-estimating the density (the average value for f was 1.21 for P78 to P103). After P104, the MG input climate factors were updated to account for actual observations made over the previous orbits. Initially, the density predictions were reasonably accurate. However, thereafter the average f-value was 0.73 from P111 to P178 indicating that the model was over-estimating the atmospheric density. Figure 5 summarizes these results.

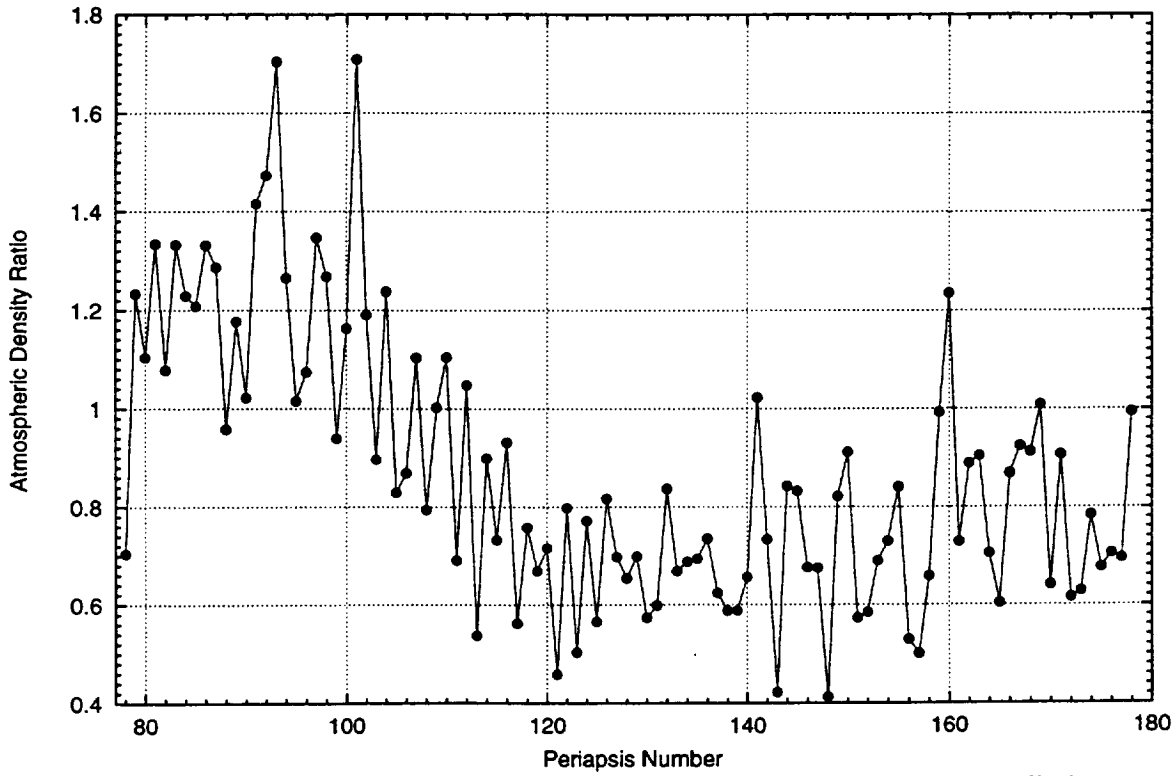

Figure 5 Atmospheric Density Ratio Used To Evaluate MG Model Predictions, Trend The Density And Generate A Three-Orbit Running Mean f-Ratio.

When this density ratio was plotted against the east longitude of the periapsis-passage location, a periodic trend was evident and unexpected. As shown in Figure 6, peaks occurred near 90 deg and 270 deg east longitude. We believe these are partially associated with the gross topography of Mars which also exhibits highs near these longitudes. This longitude dependence became an important tool for predicting densities, thus providing more accurate predictions over several orbits.

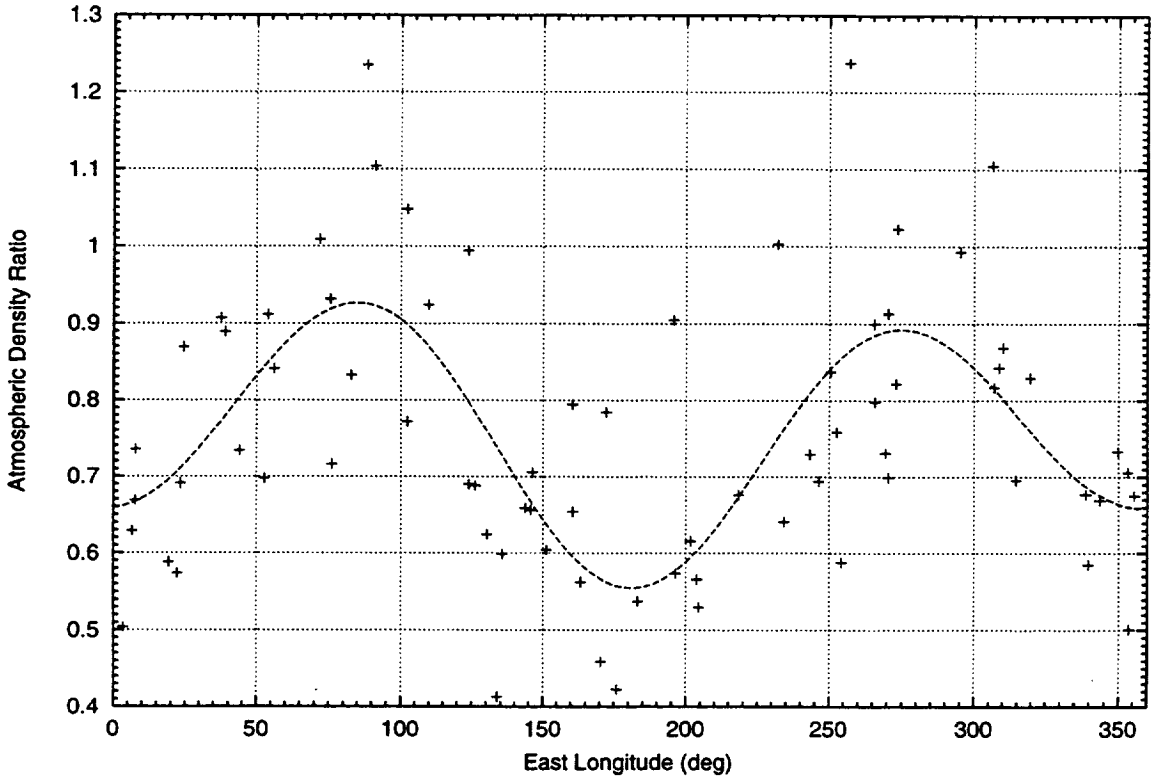

Figure 6 Periodic Trend Evident In The Density Ratio When Plotted As A Function Of The Longitude Of The Periapsis-Passage Location.

TERMINATION OF PHASE 1 AEROBRAKING

The objective of the exit ABM was to establish the SPO with a) an orbital period of 11 hr 38 min 30 sec (= 11.642 hours, osculating period at apoapsis) with a tolerance of 1 min 30 sec and b) a periapsis altitude of 170.0 km with a tolerance of 3.0 km. This maneuver was nominally targeted for A199 and once designed could not be updated. This period was selected in order to avoid ground track repeat patterns at nearby periods of 11.664 hours and 11.588 hours. Criteria for the selection of the periapsis altitude included a) consensus input by the scientists for optimal observations, b) be outside the atmosphere to avoid or minimize drag perturbations, and c) minimize the propellant required to reach this altitude. Due to fluctuations in the atmospheric density from periapsis to periapsis and the necessity of executing the final maneuver at a precise orbital period, a "walk-out" of the atmosphere was executed as shown in Table 5. This resulted in the exit ABM being executed at A201 instead of A199. In addition to increasing hp, this maneuver also increased the orbit period by 1.9 min as shown in Figure 4. Targeted and achieved SPO elements are given in Table 6.

Table 5
WALK-OUT ABMs EXECUTED TO END AEROBRAKING

Apoapsis and ABM		Velocity-Change Magnitude (m/sec)	Resultant Periapsis Altitude (km)	Atmospheric Density and Dynamic Pressure at Periapsis (kg/km^3; N/m^2)
191	ABM-49	0.09	118.0	22.4; 0.24 at P192
193	ABM-50 +	0.17	119.8	14.8; 0.16 at P194
194	ABM-51	0.33	123.4	9.5; 0.10 at P195
201	ABM-52	4.43	170.7	0.08; 0.00 at P202

Table 6
SCIENCE PHASING ORBIT TARGETING RESULTS

Orbit Element	Target Value For A199 ABM	Target Value For A201 ABM	AchievedValue
Period, hr:min:sec	11:38:30	11:38:24	11:38:38
Periapsis altitude, km	170.0	170.58	170.7

NAVIGATION CAPABILITY COMPARED TO REQUIREMENTS

Navigation easily satisfied the two major requirements (predict Tp $\leq$ 225 sec and predict hp $\leq$ 1.5 km) for all orbits from MOI to the end of AB. This was monitored by accurately determining or reconstructing the Tp (accuracy $\leq$ 0.1 sec) for each of the 201 orbits by the doppler analysis strategy previously mentioned. For each analysis, at least five predicted orbits were generated. Differences, such as Tp(reconstructed for orbit n) minus Tp(reconstructed for orbit n-1 but predicted one orbit ahead to orbit n), were plotted as shown in Figure 7. Almost all these differences are less than 2 sec with a few as high as 4-6 sec. As the period reduction became smaller, the predicted Tp accuracy correspondingly improved. A similar analysis was made for hp with the results given in Figure 8. All of the single orbit predictions are within 0.1 km of the known or reconstructed altitudes at periapsis-passage. For two orbit predictions, the Tp accuracy was within $\pm$500 seconds (except for five predictions) for orbits 1 through 100 and within $\pm$200 seconds (except for three predictions) for orbits after 100. The hp accuracy was within $\pm$0.1 km for all two-orbit predictions. Note that over this time interval, the latitude of periapsis-passage varied from 32.1 deg to 61.0 deg North and the orbit period was reduced from 45.0 to 11.64 hours.

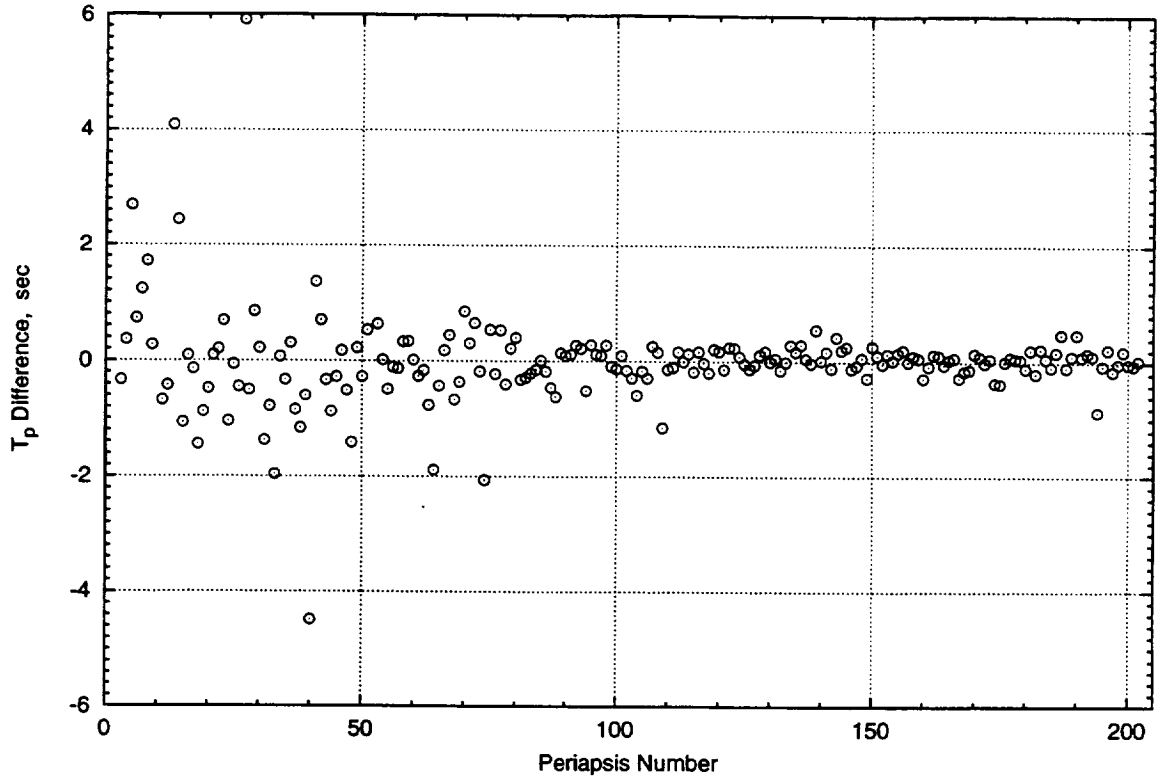

Figure 7 Accuracy Of Tp Predictions When Predicting One Orbit Ahead.

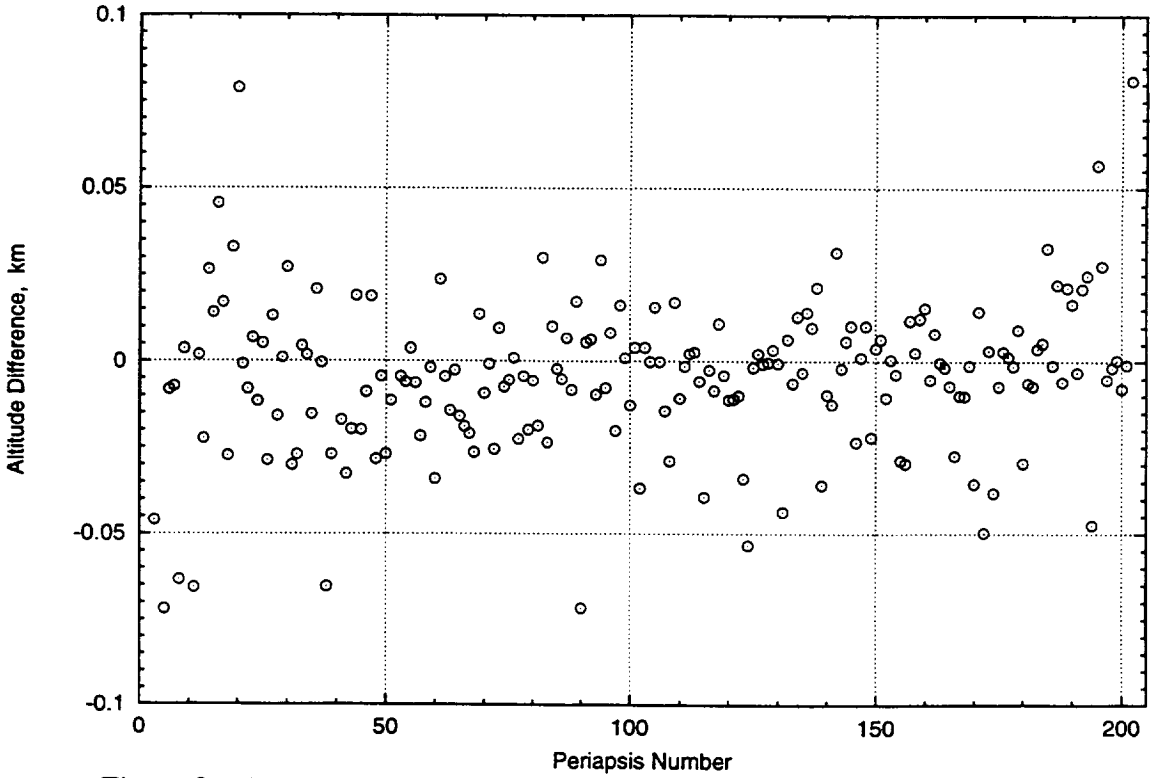

Figure 8 Accuracy Of The Periapsis Altitude, hp, Predictions When Predicting One Orbit Ahead.

ACKNOWLEDGMENT

The work described in this paper was performed at the Jet Propulsion Laboratory, California Institute of Technology, under contract with the National Aeronautics and Space Administration.

The Navigation Team gratefully acknowledges the support and interaction with many members of the MSOP flight team, both at JPL and the Lockheed Martin Astronautics facility at Denver, CO.

REFERENCES

1. P. Esposito et al, "Navigation and the Mars Global Surveyor Mission," Proceedings of the 12th International Symposium on Space Flight Dynamics, ESOC, Darmstadt, Germany, 2-6 June 1997.

2. M. D. Johnston et al, "Mars Global Surveyor Aerobraking at Mars," AAS/AIAA Space Flight Mechanics Meeting, Paper AAS 98-112, Monterey, CA, 9-11 Feb 1998.

3. M. Dornheim, "Crooked Solar Wing Forces MGS Aerobraking Changes," Aviation Week and Space Technology, p. 26, 15 Sept 1997 and B. Smith, "Solar Panel Problem Triggers Major MGS Assessment, "Aviation Week and Space Technology, pp. 25-27, 20 Oct 1997.

4. A. Konopliv and W. Sjogren, The JPL Mars Gravity Field, Mars 50c, Based Upon Viking and Mariner 9 Doppler Tracking Data," JPL Publication 95-5, Feb 1995.

5. C. G. Justus et al, "A Revised Thermosphere for the Mars Global Reference Atmospheric Model (Mars-GRAM Version 3.4)," NASA Technical Memorandum 108513, Marshall Space Flight Center, July, 1996.

6. T. Sterne, *An Introduction to Celestial Mechanics*, Interscience Publishers Inc., New York, 1960, pp. 158-160.

7. A. Seiff and D. Kirk, "Structure of the Atmosphere of Mars in Summer at Mid-Latitudes," J. Geophysical Research, Vol 2, No 28, pp. 4364-4378, 1977.

8. G. Keating et al, " The Structure of the Upper Atmosphere of Mars: In Situ Accelerometer Measurements from Mars Global Surveyor," Science, Vol 279, pp. 1672-1676, 13 March 1998.